Optimal distributed generation placement strategy to enhancing resilience against smoke effect

NAVID JAVIDTASH[1], **MASOUD JABBARI**[1,*], **TAHER NIKNAM**[1], AND **MEHDI NAFAR**[1]

[1] *Department of Electrical Engineering, Marvdasht Branch, Islamic Azad University, Marvdasht, Iran*
[*] *Corresponding author: jabbari@miau.ac.ir*

Manuscript received 15 April, 2020; revised 01 December, 2020; accepted 05 December, 2020. Paper no. JEMT-2004-1236.

Climate change raises natural disasters, especially high impact low probability (HILP) events like wildfire. The effect of wildfire on power systems could be investigated based on the flame and smoke of wildfire. Smoke can affect power system resilience, however, this effect on the power system has not yet been fully investigated. In this paper, at first, the smoke effect has been examined, and after that power system resilience has been improved by the optimal placement of distributed generation resources. Since the smoke effect depends on the direction of the wind, and it has stochastic nature, the wind rose curve has been used to reduce possible scenarios. It should be noted that the proposed method has been studied on the IEEE 33-bus distribution system to the multi-objective placement of distributed generation sources. Since the multi-objective solutions have Pareto set answers, it is provided to find a unique answer by using the fuzzy method. Also, a new optimization algorithm has been presented for the first time that is called the handball championship cup algorithm or HCCA algorithm. It is shown that the proposed methods have good accuracy, and are suitable for improving the power system resilience against the smoke effect.

keywords: *Power system resilience, Smoke effect, Distributed generation sources placement, HCCA algorithm*

http://dx.doi.org/10.22109/jemt.2020.226576.1236

NOMENCLATURE

E_{rm} Electric field strength [v/m]
E_0 Electrical field without particles[v/m]
$\boldsymbol{r}$ Distance away from the center of the particle [m]
$E_{1,2}$ Electric field strength of r direction around the particle [v/m]
T_c Constant empirical coefficients [k]
Z_p Constant related to flame height [m]
Z_d Constant related to fuel height [m]
$\boldsymbol{K}$ Empirical constant
T_{fl} Decrease in temperature with height in the fire plume [k]
$\boldsymbol{D}$ Diameter of particle[m]
N_{obj} Number of objective functions
R_i Resistance of the ith branch of the test power system [Ω]
I_i Current of the ith branch of the test power system [A]
N_{br} Total number of branches of test power system
C_i Price of fuel [$/kWh]
P_s Active power generated at the substation bus of distribution feeders [kW]
C_s Cost coefficient of the substation bus [$/kW]
$C_{L.SH}$ Cost of blackout damages caused by disconnected from the network in the studied area [$/kWh]
$P_{L.SH}$ Energy not supply in the mentioned area in the event of a blackout, or cost of social Effect [kWh]
N_{DG} Number of DGs
$\boldsymbol{N}$ Number of buses
V_i Voltage of the i'th bus bar of the test power system [V]
V_{rating} Nominal voltage [V]
NO_x Emission coefficient [lb/MW]
CO_x Emission coefficient [lb/MW]
SO_x Emission coefficient [lb/MW]
$\boldsymbol{M}$ Number of generator
V_k Voltage of kth bus bar [V]
V_{min} Minimum allowed voltage that is equal to 0.95 Per Unit
V_{max} Maximum allowed voltage that is equal to 1.05 Per Unit
P_G Total generated active power in the test power system [kW]
P_{load} Total active power of loads in the test power system [kW]
P_{loss} Total active losses in the test power system [kW]

$P_{DG,i}$ Generated power by the ith distributed generation resources [kW]

$P_{DG,max,min}$ Maximum/Minimum DG Capacity [kW]

$\propto$ Coefficient, that $0 < \propto (i) < 1$

f_u Utopia point in fuzzy membership function

f_n Nadir point in fuzzy membership function

f_{SN} Pseudo nadir point

Ω Feasible region of cost functions

w_n Weight coefficient of nth objective function

M Number of answers in Pareto set

1. INTRODUCTION

In light of modern life, an increase in electricity usage is an unavoidable fact. It is expected that the world's power consumption will rise by 53% by 2035 [1] and as a result of that power grids infrastructure increase very fast in the world. On the other hand, climate change and human appetite are increasing greenhouse gas emissions have increased the natural hazards, hence power systems could be exposed to high- impact low probability (HILP) phenomena, that this base of power system resilience analysis. So identifying the nature of different phenomena can provide proper planning background to reduce the effects of events [2, 3]. In natural disasters, designed and planning engineering techniques, and strategies that are used to keep the stability of the power system in the operating mood. However many challenges and constraints should be considered to improve power system resilience [4]. In [5] is expressed that according to the National Infrastructure Advisory Council report, resilience contains robustness, resourcefulness, rapid recovery, and adaptability. Also, some resilience enhancement methods like using distribution automation technologies [6], defensive islanding [7], mobile emergency generator [8], optimal switch placement in distribution systems [9], and transportable energy storage systems [10] can be deployed to make power grids more resilient. In [11] different hardening proceedings, like vegetation management are integrated into a tri-level optimization problem for the optimization of the hardening investment and the projected load shedding cost under extreme weather conditions. In [12] to power grid resilience improvement against cascading events that are caused by line damages in extreme weather situations an islanded layout is proposed. In [13] the main purpose is to specify the causes of widespread blackouts and finding approaches to enhancement of the system against extreme weather. In [14] shows that the nature of natural disaster blackouts is different from the nature of internal failures in electrical systems. So, long time restoration is needed. In [15] in terms of continuous load distributed generation sources have been optimized. In [16] smoke effect of three plant species on electrical insulators has been tested. It shows how the nature of smoke can cause insulation failure. In [17] a test has been designed to obtain the failure voltage caused by smoke that is compared in non-smoke and smoke conditions. Also, the experimental space was tested and analyzed by AC and DC fields and the effects of those are mentioned. In [18] optimizing operating power systems against wildfire as resilience, the scenario has been evaluated. However, because of the focus on the flame and lack of attention to the smoke of wildfire, only one scenario is provided. In [19] by constructing and installation of appropriate resiliency sources the resiliency-based power system expansion planning can improve the resiliency index. Also, resiliency sources show the network equipment which is not disconnected from the power system during natural disasters. So In weather extreme conditions, they can improve the power system flexibility and keep it in the operating mood. In [20], a Monte Carlo simulation method and a fragility model-based framework for resilience are presented. The remarkable point is that by using reliability indices such as Loss of Load Frequency, Expected Energy Not Supplied, and infrastructure indices, the system resilience against extreme weather situations has been estimated. In [21] an approach to estimate the damage caused by wildfire to the distribution system is proposed. But, no strategy is presented to overcome the threat of the fire. In [22] the effect of a progressing wildfire online ratings of a power system is presented, also and an optimal power flow technique is proposed to reduce line capacities due to the wildfire. In [23] and [24] a new approach for an optimal distribution system operation against the flame of wildfire in attendance of microgrids is presented. Considering resilience it seems that optimal placement of devices in the power system can increase the satisfaction of end-users and players of electricity markets [25]. In [26] performance of Microgrids has been improved by using coalition game theory to optimal placement of distributed generation sources. In [27] has been tried to find a new index based on power stability to find the best place of distributed generation sources. In [28] impact of combination between shunt capacitor and distributed generations on the placement of DG's has been investigated. In [29] and [30] with special attention to power system constraints, placement of distributed generation sources has been achieved by using Particle Swarm Optimization and Genetic Algorithm methods. One of the most inclusive disasters is large wildfires that can enter serious damages to power grids. Thus taking necessary arrangements such as using distributed generation sources at risk points can reduce the consequences of possible damages.

In this paper by considering that in case of wildfire near the power system, large volumes of smoke are released, how to increase power system resilience against smoke effect by optimal placement of distributed generation resources will be investigated. It should be noted that the smoke releasing by wind has stochastic nature, so the various scenarios arising from this phenomenon have been investigated and the most optimal decision based on it is adopted. Thus in this paper by using the wind rose curve as an innovative method, the most effective scenarios are identified. Also to analyze multi-objective problems, many algorithms have been provided so far, but in this paper, a new algorithm that is based on the handball championship cup is presented for the first time. The remainder of this paper is organized as follows:

The second section presents a description of the proposed methods. The third section makes it possible to show the ability of proposed methods by numerical analysis. After that in the fourth section, the results are discussed, and finally, the main conclusions section is presented.

2. DESCRIPTION OF PROPOSED METHODS

A. Smoke effect

The wildfire has contributed to human civilization in history and has also had serious damage, therefore, the fire has always been one of the common issues researched by researchers [31–33]. Fire contains two factors of smoke and flame, which can vary depending on the material of burning. Uncontrolled vegetation like cane is one of the most common causes that can happen near power transmission lines. The event is mostly occurring in countries where the rate of vegetation is more, also climate change of recent years has increased destructive wildfire. In the case of wildfire both flame and smoke, can be harmful to the power systems. If the flame reaches a small distance from the power lines, it may cause serious damage, however, the wildfire smoke can lead to an insulation failure on the winding path. The major difference between flame and smoke is that in the event of wind the spread speed of smoke will be much higher than the flame and the smoke in a very little time can reach the power system. The effect of smoke on power system and the possibility of insulation failure is undeniable.

As shown in Fig. 1, smoke caused by natural resources wildfire contains inorganic particles that because of fluidity and the speed of smoke emission release, this is an effective issue on the power system performance. The vertical temperature of wildfire is variable based on the inorganic plume height. Also in Fig. 2, the influence of natural resources wildfire in the near a power system is shown. It can be found that the impact of inorganic particles on the electric field distribution is remarkable, where E_0 is the background electric field strength without inorganic particles in the gap, and Ex is the electric field strength with particles in the gap. Also, the electric field appears sharp enlargement at both ends of the particle, and the closer the distance between the particle and conductor, the greater the electric field strength is, and thus it is easy to trigger discharge in the process of particles near the conductor [16, 17]. The following equations are considered for the mentioned cases.

$$T_{fl} = T_c + K * exp\left(\propto_f (z - z_d)^2\right) \quad (1)$$

$$\alpha_f = 1/(2z_p(z_p - z_d)) \quad (2)$$

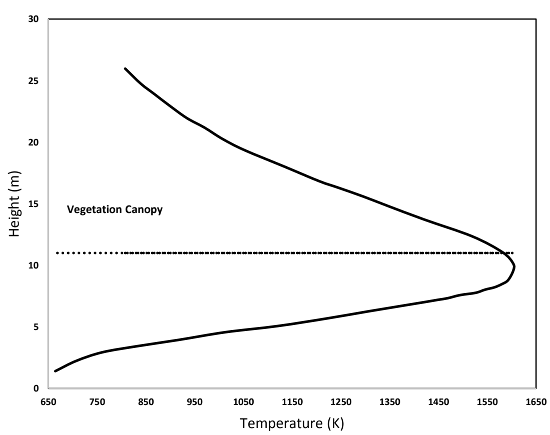

Fig. 1. Temperature of smoke in the height of the flame [16].

Also, for non-uniform fields of suspended particles in smoke can be written:

$$E_{rm} = E_{r1} + E_{r2} \approx (1/D^3 + 4r^3)E_0 + 3(D^2 + 4r^2)E_0 \quad (3)$$

B. Wind rose curve; an innovative approach for scenario reduction

Wildfire and smoke propagation in the geospatial environment is a condition that accompanies uncertainty, that this is more important for a smoke since smoke emissions are faster and

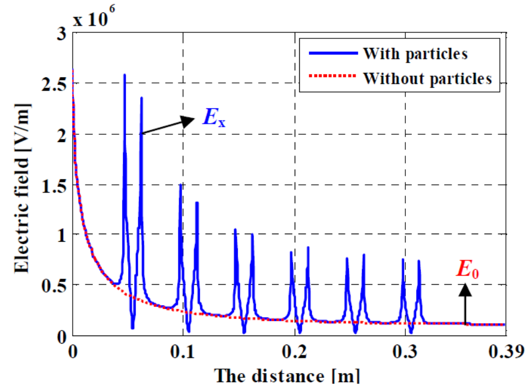

Fig. 2. Non-uniform fields resulting from suspended particles in fire smoke [17].

more likely. There are different methods for uncertainty analysis, such as:

In stochastic programming, based on fuzzy logic, each of the variables has an uncertainty of a fuzzy membership function. Usually, this membership function is considered normal. Also, the cost functions of the optimization issue are also modeled with a membership function that is often considered to be a trapezoidal image [34].

Monte Carlo method is one of the most accurate methods of stochastic analysis [35]. Monte Carlo method with a random sampling of the distribution function of random variables attempts to resolve the issue by considering the number of existing uncertainties. The main problem of Monte Carlo is its very heavy computational load. The accuracy of the Monte Carlo method is dependent on the number of examples that the distribution functions choose. The higher the number of samples, the calculation accuracy, and the computational load will be higher. In this method, the behavior of the issue will be achieved by considering the specific input distribution functions. Although the Monte Carlo method is the strictest stochastic planning method, the high computational volume of this method has led to a great deal to solve practical issues. Other methods are designed based on the concept of Monte Carlo to slow down the balance between precision and computational load. Two groups of these methods are random programming based on scenario formation and other estimated methods. The superiority of each of these two groups is different depending on the issue studied [36].

In solving stochastic programming issues, it has to be possible to transform the uncertain issue into a number of definite issues and then solve it. Somehow the results obtained from the definitive equivalent stuff reached a random issue response. In the generation of a scenario, each of the definite states is called a scenario [37].

The first step in solving stochastic issues modeling the variables is the uncertainty of the issue. Modeling the distribution functions of random variables in power grids such as loads are carried out by continuous distribution functions. Continuous distribution functions can generate a myriad of different and different modes for a potential network situation. For example, a sample point of the load distribution function in a specified hour can be associated with all parts of the load distribution function in the next hour. Implies that all gestures may not be possible. Therefore, in random planning, based on scenario generation, the distribution function of random variables is distributed.

After the wildfire is used to scatter the smoke into geographic characteristics and direction of the wind, since the direction of the wind is a stochastic nature, therefore, to evaluate the impact of smoke on the electricity network, the use of computational methods will be complicated with considering all the possibilities of stochastics. Therefore, in order to reduce the existing scenarios, the wind rose curve can be used. The wind rose curve shows how likely the wind direction will occur and it has been used in many types of research [38–42]. Therefore, using the possible path of the wind and considering GIS information, it is possible to estimate the potential location of smoke influence on the electricity network, for example, the wind rose curve, are in Fig. 3 [43].

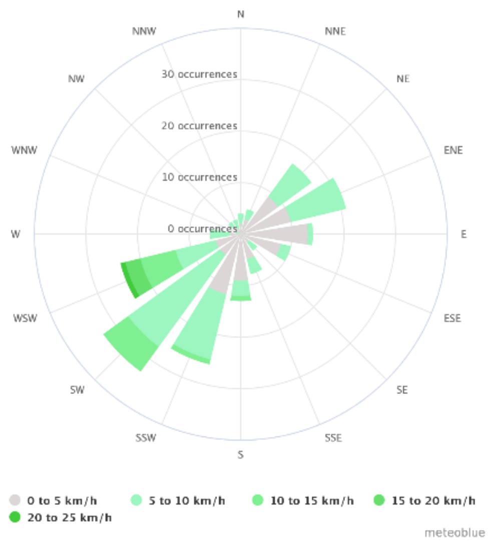

Fig. 3. Wind rose curve.

C. A new multi-objective optimization algorithm: Handball Championship Cup Algorithm:

Multi-objective optimization based on classic methods (such as weighted sum, e-constraints, goal programming, etc.) are very slow because, in every iteration, the algorithm should run equal to the number of objective functions, but in the Pareto front method, the framework of the algorithm has been designed based on domination set, so as general x_1 dominate x_2 if:

$$\forall i \in \left\{1, 2, \ldots, N_{obj}\right\} : f_i\left(X_1\right) \leq f_i\left(X_2\right) \quad \textbf{(4)}$$

$$\exists j \in \left\{1, 2, \ldots, N_{obj}\right\} : f_j\left(X_1\right) < f_j\left(X_2\right) \quad \textbf{(5)}$$

Handball is a fast-paced team game that was first played in Scandinavia and Germany at the end of the 19th century; however, handball competitions have been changed during decades. Today, the handball championship cup is held every two years and 24 teams compete with each other in four categories. At first, the group competition step is held and after those four teams of each group go to the knockout stage, and finally, the winner of all knockout competitions will be champions.

It should be mentioned that after each competition, winner and loser teams try to recovery and improved themselves for the next competition, also winner and loser teams have positive and negative moods respectively. Every team in handball has a captain that is the best player among all of the players. How to group and flowchart of the proposed algorithm have been presented in Figs. 4 and 5, respectively [44].

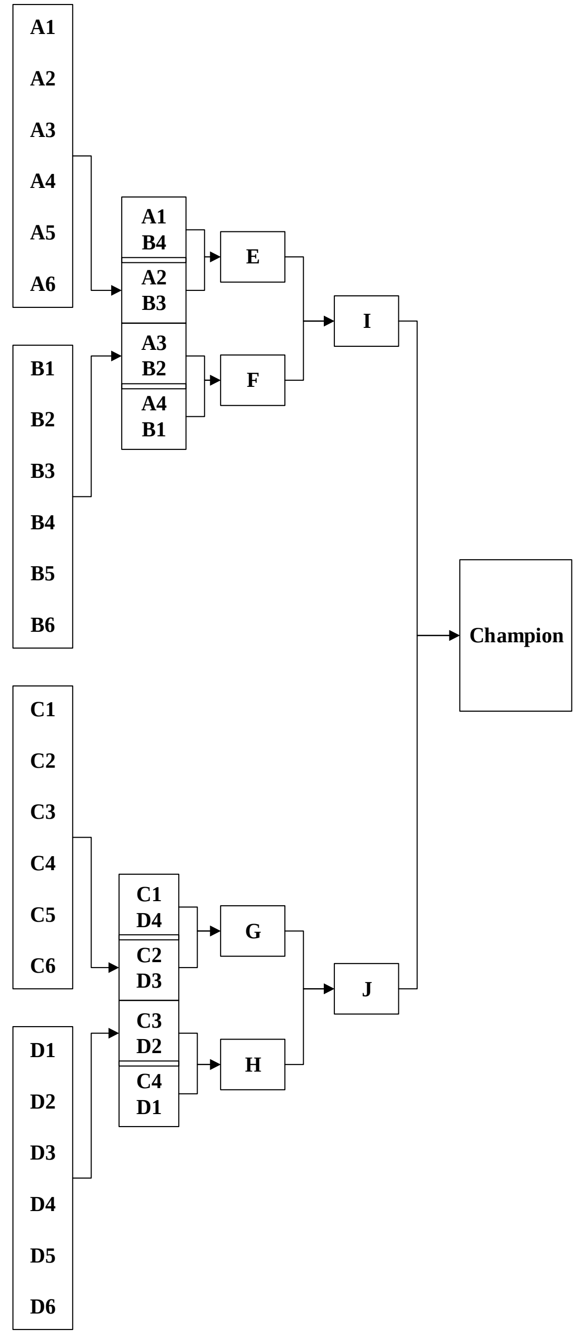

Fig. 4. Tournament plans of handball championship cup.

In the initializing step initial data such as network data, number of distributed generation sources, number of players, stop criteria and etc. are entered, then each of the players will draw through randomly in one of the teams.

$$Team_i = \left[Player_1, Player_2, \ldots, Player_n\right] \quad \textbf{(6)}$$

$$Group\left(A\right) = \left[Team_1, Team_2, \ldots, Team_n\right] \quad \textbf{(7)}$$

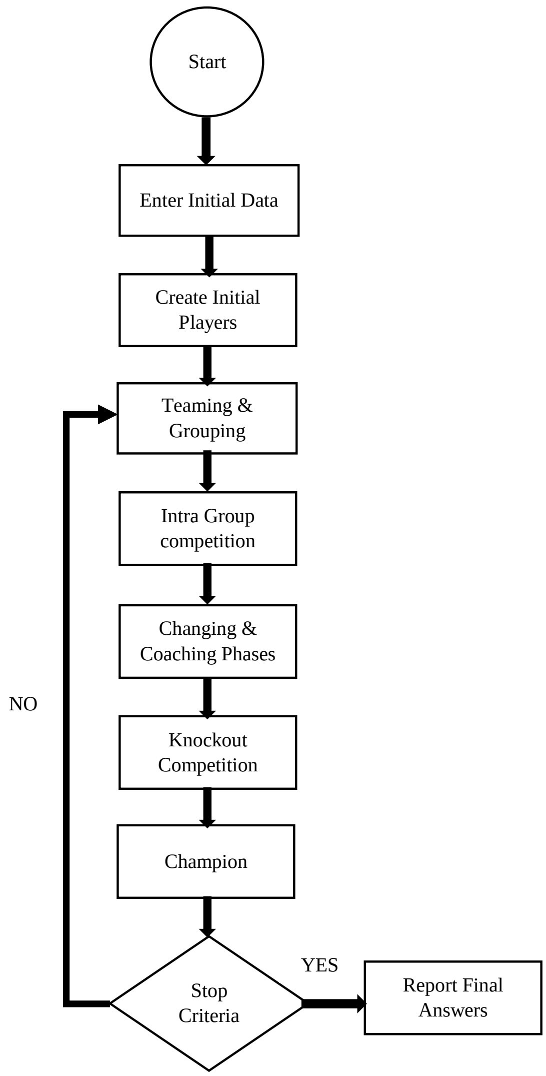

Fig. 5. Flowchart of HCCA algorithm.

In the next step, the captain will be selected among team players.

$$PlayersCost = Evaluate\left(Team_j\right) \quad (8)$$

$$BestPlayers = non - DominatedPlayersofTeam_j \quad (9)$$

$$Captain_j = random\left(BestPlayersofTeam_j\right) \quad (10)$$

In intragroup competition, each of them has a tournament with another teammate and the team wins 4 points. In the next step, three teams of each group enter the knockout competition. With the continuation of this process, the winner of the championship cup is determined. It should be mentioned after each competition changing and coaching phases are applied.

In changing (substitute) and coaching steps, after each tournament, the winning team could eliminate bad players and instead of them with a copy of good players of loser teams. It should be noted that the number of copied players could be changed based on changing factors.

After each tournament winner and loser teams try to analyze and improve themselves, thus to implement this factor using different methods is possible because different methods could change the quality of answers. In this paper, since the captain is equal to the coach, after each tournament and doing the changing step, the captain of the team should be found and other players have been changed by the captain. Thus by using the coaching phase answers should find global optimum instead of local optimum by correcting the position of players and applying stochastic changes.

It should be mentioned, in the changing phase, the maximum number of players that could be changed is equal to half of each team player and in the coaching phase, different methods can be used. In the presented version of the HCCA algorithm, the coaching phase is inspired by the teacher's phase in the TLBO algorithm, that here the captain acts as a teacher. Also, analysis benchmark functions to show the ability of the HCCA algorithm has been presented in the appendix section.

D. Fuzzy method

The membership function of the fuzzy method is as follow:

$$\mu_{f_i} = \begin{cases} 1 & for\ f_i(X) \le f_i^{min} \\ 0 & for\ f_i(X) \ge f_i^{max} \\ \frac{f_i^{max} - f_i(X)}{f_i^{max} - f_i^{min}} & for\ f_i^{min} \le f_i(X) \le f_i^{max} \end{cases} \quad (11)$$

In the fuzzy membership function, the continuous value between 0 and 1 for lower and upper boundaries is calculated. But before that for calculating the f_{i-min} and f_{i-max} pay-off table should be established [45].

Before creating the Payoff table matrix, single-objective optimization for each of the cost functions is calculated separately, after that the best point of each cost function is calculated for other cost functions in the Payoff table matrix and finally the best and the worst answer of each objective function is known as a utopia point (f_U) and nadir point (f_N) as follows:

$$\Phi = \begin{pmatrix} f_1^*(\bar{x}_1^*) & \cdots & f_i(\bar{x}_1^*) & \cdots & f_p(\bar{x}_1^*) \\ \vdots & \ddots & & & \vdots \\ f_1(\bar{x}_i^*) & \cdots & f_i^*(\bar{x}_i^*) & \cdots & f_p(\bar{x}_i^*) \\ \vdots & & & \ddots & \vdots \\ f_1(\bar{x}_p^*) & \cdots & f_i(\bar{x}_p^*) & \cdots & f_p^*(\bar{x}_p^*) \end{pmatrix} \quad (12)$$

$$f^U = \left[f_1^U, ..., f_i^U, ..., f_p^U\right] = \left[f_1^*(\bar{x}_1^*), ..., f_i^*(\bar{x}_i^*), ..., f_p^*(\bar{x}_p^*)\right] \quad (13)$$

$$f^N = \left[\ f_1^N,\ \ldots,\ f_i^N, \ldots,\ f_p^N\right] \quad (14)$$

So to minimize the objective functions:

$$f_i^N = \max_{\bar{x}} f_i(\bar{x})\ , \text{subjectto} \bar{x} \in \Omega \quad (15)$$

$$f^{SN} = \left[\ f_1^{SN},\ \ldots,\ f_i^{SN}, \ldots,\ f_p^{SN}\right] \quad (16)$$

$$f_i^{SN} = \max\left\{f_i(\bar{x}_1^*), ..., f_i^*(\bar{x}_i^*), ..., f_i(\bar{x}_p^*)\right\} \quad (17)$$

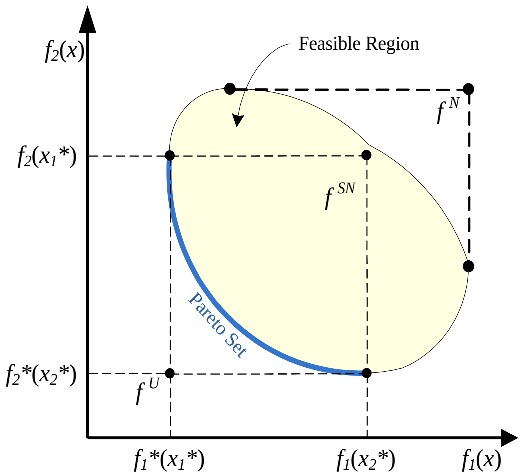

Fig. 6. Utopia point, nadir point, and pseudo nadir point.

Utopia point, nadir point, and pseudo nadir point are shown in Fig. 6 for two objective functions.

Finally, when utopia points and pseudo nadir points have been calculated, the total membership function is calculated as follow:

$$\mu^k = \frac{\sum_{i=1}^{p} w_i.\mu_i^k}{\sum_{k=1}^{M}\sum_{i=1}^{p} w_i.\mu_i^k} \tag{18}$$

The system operator could choose the best mode in different circumstances for the power system by changing w_n. For example, if in some circumstances security is the most important item for the operator, the weight coefficient of it could be increased in comparison with other items. Flowchart of the fuzzy method has been presented in Fig. 7.

3. NUMERICAL ANALYSIS

To implement the proposed method, the sizing of 8 distributed generation sources for a 33 buses IEEE standard network [46], which has already been sitting by sensitivity analysis has been considered. Characteristics of distributed generation resources have been presented in Table 1, also four objective functions are considered such as total cost, emission, voltage deviation, and losses [47, 48].

A. Objective functions

The cost function of distributed generation resources and social cost resilience

Cost is one of the most important motivational factors in selecting the type of distributed generation resources by investors. This issue of initial investment costs started and based on the type and technology of resources, including fixed and variable costs, which ultimately cost function for different power plants is defined as follows:

$$\text{Cost} = (C_{L.SH} \times P_{L.SH}) + \sum_{i=1}^{N_{DG}} C_{DG,i} + C_{substation} \tag{19}$$

$$C_{DG,i} = 1.3 \times FixedCost + VariableCost \tag{20}$$

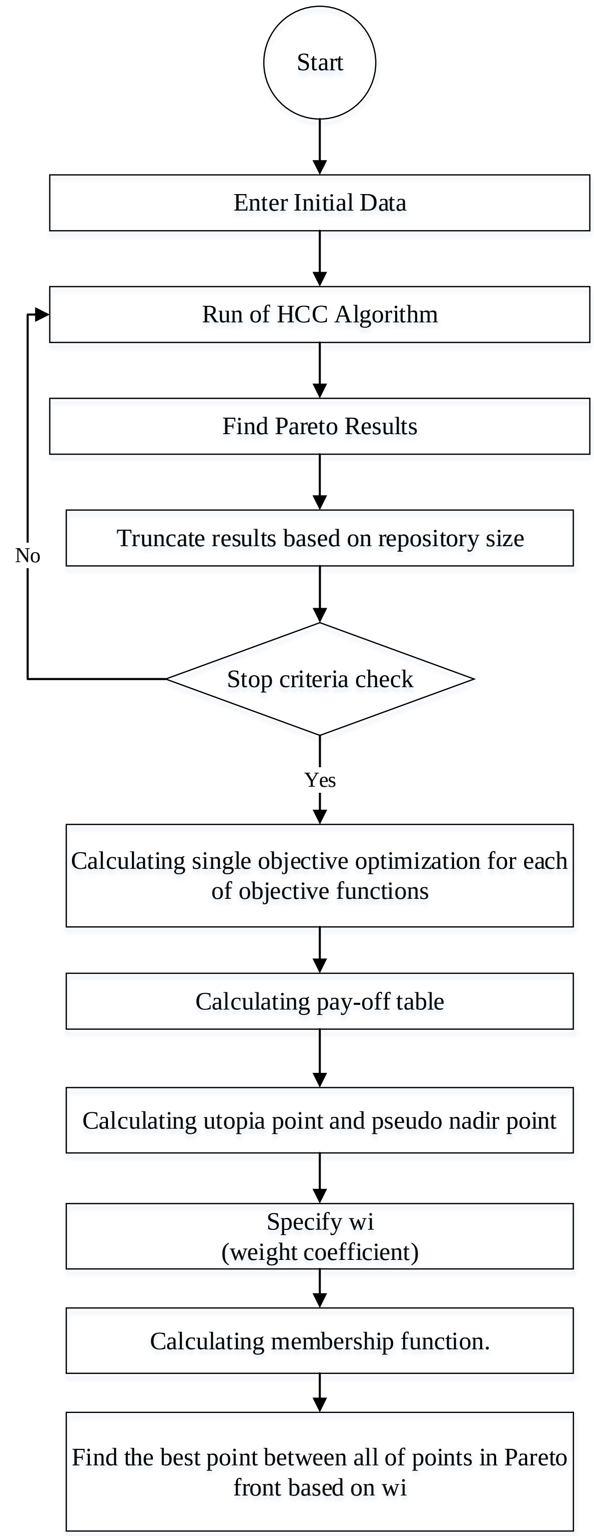

Fig. 7. Flowchart of the fuzzy method implementation.

$$FixedCost = CapitalCost \times MaximumCapacityofDG \tag{21}$$

Table 1. Characteristics of distributed generation resources [47, 48].

DG Type	Operation and maintenance costs (\$/KWh)	Fuel cost (\$/kW)	Cost of investment (\$/kW)	Capacity (kW)	Emission coefficient (lb/MW)		
					COx	SOx	NOx
Wind turbine	0.2	0	800	100	-	-	-
Micro turbine	0.5	0.104	700	500	1596	0.008	0.44
Fuel cell	0.7	0.02	3500	200	1108	0.008	1.15
Solar cell	0.3	0	4500	150	-	-	-

$$VariableCost = (FuelCost + OperatingandmaintenanceCost) \times P_{DG,i} \quad (22)$$

$$C_{Substation} = P_s \times C_s \quad (23)$$

$$f1 = min[Cost] \quad (24)$$

Where, P_s is the active power generated at the substation bus of distribution feeders and C_s is the cost coefficient of the substation bus.

Voltage Deviation

To calculate voltage deviation can write the following formula:

$$Voltage - Deviation = \sum_{i=1}^{N} \frac{\left|V_{rating} - V_i\right|}{V_{rating}} \times 100 \quad (25)$$

$$f2 = Min[Voltage - Deviation] \quad (26)$$

Losses

To calculate the amount of losses between the lines of a power grid the following equation can be used:

$$Losses = \sum_{i=1}^{N_{br}} (R_i \times \left|I_i^2\right|) \quad (27)$$

$$f3 = min\,[Losses] \quad (28)$$

Emission

To calculate the amount of emission, considering atmospheric pollutants such as sulfur oxides (SO_x), carbon oxides (CO_x) and nitrogen oxides (NO_x) can be evaluated, which is often considered as a CO_2 effect on power plants. The formulation of emission can be expressed as follow:

$$E_{DG,i} = (NO_X^{DG,i} + SO_2^{DG,i} + CO_2^{DG,i}) \times P_{DG,i} \quad (29)$$

$$E_{Grid} = (NO_X^{Grid} + SO_2^{Grid} + CO_2^{Grid}) \times P_s \quad (30)$$

$$f4 = min\,[Emission] \quad (31)$$

B. Constraints

Important and influential constraints on the analysis of sizing distributed generation resources in the assumed power grid can be expressed as follows:

B.1. Voltage constraint

$$V_{min} \leq |V_k| \leq V_{max} \quad (32)$$

B.2. Power generation constraint

$$\sum P_G = \sum (P_{load} + P_{loss}) \quad (33)$$

$$P_{DG,maxd} \leq P_{DG,i} \leq P_{DG,min} \quad (34)$$

B.3. Maximum allowable capacity of each feeder

It must be taken into account that when DG units are considered, the total DG size for each feeder should be governed by the following equation:

$$\sum_{i=1}^{N_{DG}} P_{DG,i} \leq \propto (i)\, P_{Load} \quad (35)$$

$$0 < \propto (i) < 1$$

Where In this article, the value of $\propto$ (i) = 0.4 has been calculated [47].

C. Case study simulation results

To demonstrate the performance of the proposed method, at first, a region full of straw near 33 buses is assumed, and wind condition is like Fig. 8, so by using GIS, scenarios, and zones of the power system that can be damaged by smoke effect in conditions of fire are recognizable, that is presented in Table 2. Also based on three calculated scenarios, the sitting of DGs are presented in Table 3.

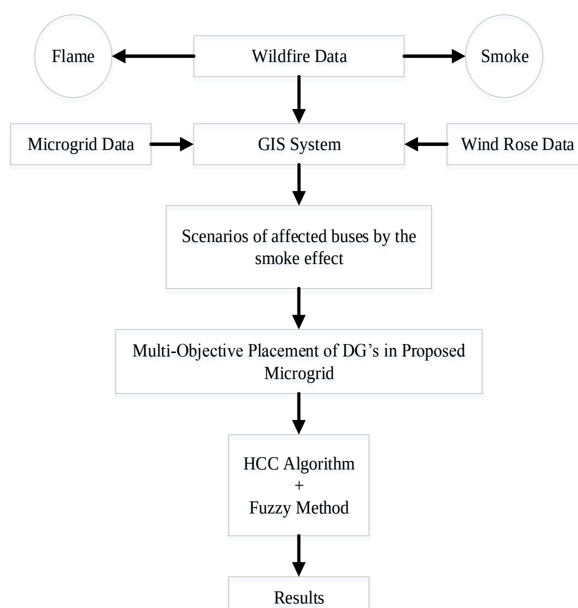

Fig. 8. Flowchart of proposed method.

Table 2. Affected zones by smoke.

Zone number	Probability	Bus number		Load shedding (kW)
		From	To	
1	18%	30	32	420
2	15%	23	25	930
3	11%	15	18	270

For the first scenario, the acceptable convergence characteristic of objective functions has been shown in Fig. 9. Comparison between the results of the proposed algorithm with Genetic and PSO algorithms has been presented in Table 4, it obviously shows that the results of the HCCA algorithm are better than GA and PSO algorithms. Also to comparison two by two objective functions, Pareto front results that are obtained by the proposed algorithm has been shown in Fig. 10, in addition, three objective functions comparison has been shown in Fig. 11, so with regard to recent figures, diversity of calculated results despite their conflict could be shown.

Since show results of four objective functions impossible, numerical results could be presented, but in multi-objective analysis, results are not unique that is called Pareto front answers as mentioned, so by using a fuzzy method decision-maker could find the best point between Pareto answers.

In addition to showing different combinations of objective function various cases have been considered:

Cases I-IV are shown results of single-objective optimization.
Case V: Considering functions f_1, f_2, and f_3.
Case VI: Considering functions f_1, f_3, and f_4.
Case VII: Considering functions f_2, f_3, and f_4.
Case VIII: Considering functions f_1, f_2, and f_4.
Case IX: Considering functions f_1, f_2, f_3, and f_4.
According to the structure of the HCCA algorithm and fuzzy method, combination steps of them presented as follow:
As a result, the analytical table of cases for the first scenario has been presented in Table 5. Similarly, the results of the second and third scenarios have been presented in Tables 6 and 7.

4. DISCUSSION

Rising wildfires caused by climate change are a source of a new concern for power networks. Wide wildfires have two effects, smoke, and flame. However, the spread of flames can damage power grids [18], but smoke from a wildfire can show its effect in a shorter time [16]. So, considering the nature of smoke effect uncertainty, an appropriate strategy should be considered to increase the resilience of the power system by the use of distributed generation sources.

Due to the fluidity of the smoke and the direction of the wind at different times, identifying the place of its effect on the power system is uncertain. As shown in the section of simulation, the wildfire smoke could have spread in different directions that are depending on the direction of the wind, but considering the wind rose curve, the most possible directions could be identified and analyzed. As shown in Table 2, three probabilities have been analyzed, the first being the 18% probability that in the GIS system assumed, could outage the bus bars 30 to 32 with 420 kW blackout. Similarly, with a 15% probability, the area between bus bars 23 to 25 with 930 kW and 11% probability, the area between bus bars 15 to 18 with 270 kW could be a blackout. To placement of 8 DGs in the test network, it is decided that in each of the possible scenarios, the important loads of the smoke-

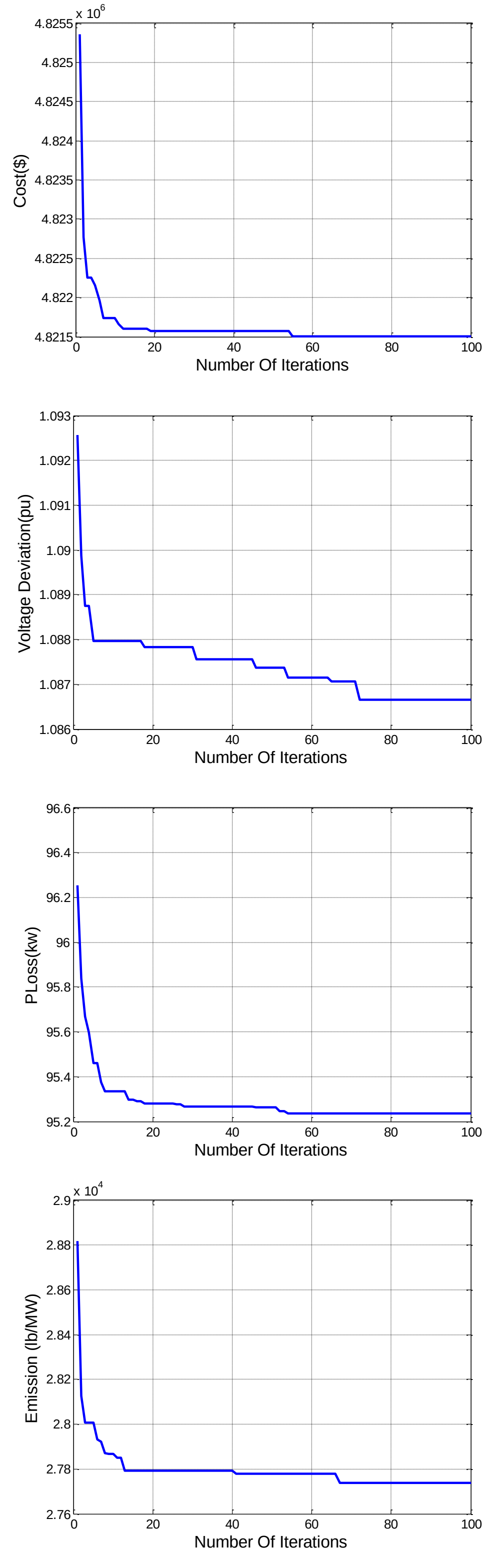

Fig. 9. Convergence characteristic of objective functions.

affected area will be provided by one or more DGs. Since the considered problem has more than one objective function, so the optimization method with a multi-objective nature should be used, which is the basis of the HCCA algorithm. To analyze the results obtained from the optimization of different combinations

Table 3. DG locations in different scenarios.

Numbr of Scenario	Bus NO. for DG1	Bus NO. for DG2	Bus NO. for DG3	Bus NO. for DG4	Bus NO. for DG5	Bus NO. for DG6	Bus NO. for DG7	Bus NO. for DG8
1	23	7	24	31	32	30	17	13
2	24	7	31	13	25	32	17	30
3	23	7	24	31	18	30	32	13

Table 4. Comparison between HCCA, GA and PSO algorithms.

Method	Function			
	$f_1 * 10^6$ ($)	f_2 (pu)	f_3 (kW)	$f_4 * 10^4$ (lb/MW)
Genetic algorithm	3.1419	109.18	0.971	4.8689
PSO algorithm	1.9817	107.99	0.913	4.849
Proposed algorithm	2.297	107.368	0.888	4.8448

Table 5. Objective function values for the first scenario.

Cases	Operational weights				$f_4 * 10^4$	f_3	f_2	$f_1 * 10^6$
	W_1	W_2	W_3	W_4	(lb/MW)	(kW)	(pu)	($)
I	-	-	-	-	4.6681	1.096	107.016	3.1016
II	-	-	-	-	4.8378	0.888	107.368	2.297
III	-	-	-	-	4.8448	0.961	96.308	2.5582
IV	-	-	-	-	5.2562	0.934	98.517	2.271
V	0.33	0.33	0.33	-	4.5583	0.95	98.51	-
	0.2	4	0.4	-	4.5583	0.95	98.51	-
	0.4	0.2	0.4	-	4.5583	0.95	98.51	-
	0.4	0.4	0.2	-	4.6237	0.92	100.6	-
VI	0.33	-	0.33	0.33	4.5583	-	98.51	2.3547
	0.2	-	0.4	0.4	4.5583	-	98.51	2.3547
	0.4	-	0.2	0.4	4.5583	-	98.51	2.3547
	0.4	-	0.4	0.2	4.5583	-	98.51	2.3547
VII	-	0.33	0.33	0.33	-	0.93	99.44	2.3717
	-	0.2	0.4	0.4	-	0.95	98.51	2.3547
	-	0.4	0.2	0.4	-	0.93	99.44	2.3717
	-	0.4	0.4	0.2	-	0.93	99.44	2.3717
VIII	0.33	0.33	-	0.33	4.6918	0.91	-	2.3869
	0.2	0.4	-	0.4	4.6918	0.91	-	2.3869
	0.4	0.2	-	0.4	4.6918	0.91	-	2.3869
	0.4	0.4	-	0.2	4.6918	0.91	-	2.3869
IX	0.25	0.25	0.25	0.25	4.5583	0.95	98.51	2.3547
	0.1	0.3	0.3	0.3	4.5583	0.95	98.51	2.3547
	0.3	0.1	0.3	0.3	4.5583	0.95	98.51	2.3547
	0.3	0.3	0.1	0.3	4.7054	0.91	101.22	2.3733
	0.3	0.3	0.3	0.1	4.5583	0.95	98.51	2.3547

as single-objective, two-objective three-objectives, and finally four-objective is considered. Table 4 shows that the introduced algorithm has found more optimal answers than the PSO and GA algorithms. Also, in the study of multi-objective optimization, a set of answers in the form of Pareto has been obtained, which show in Figs. 9 and 10. But the important thing about multi-objective optimization problems is that at first glance it is not possible to choose a unique answer between Pareto set results. In the sample problem, the network planner cannot identify a single answer from the set of answers obtained, so by combining the optimization method with the fuzzy method, it is possible to determine the importance of objective functions based on W_i

Table 6. Objective function values for the second scenario.

Cases	Operational weights				$f_4 * 10^4$	f_3	f_2	$f_1 * 10^6$
	W_1	W_2	W_3	W_4	(lb/MW)	(kW)	(pu)	($)
I	-	-	-	-	4.6733	1.13	108.87	3.1848
II	-	-	-	-	4.8831	0.98	120.96	2.7466
III	-	-	-	-	5.0074	1.08	105.29	2.9985
IV	-	-	-	-	4.7767	1.05	107.01	2.6981
V	0.33	0.33	0.33	-	4.9966	1.05	105.88	-
	0.2	4	0.4	-	4.9966	1.05	105.88	-
	0.4	0.2	0.4	-	4.9966	1.05	105.88	-
	0.4	0.4	0.2	-	4.9196	1.03	108.92	-
VI	0.33	-	0.33	0.33	5.0241	-	105.61	2.9414
	0.2	-	0.4	0.4	5.0241	-	105.61	2.9414
	0.4	-	0.2	0.4	5.0241	-	105.61	2.9414
	0.4	-	0.4	0.2	5.0241	-	105.61	2.9414
VII	-	0.33	0.33	0.33	-	1.05	105.88	2.8162
	-	0.2	0.4	0.4	-	1.05	105.88	2.8162
	-	0.4	0.2	0.4	-	1.03	108.92	2.7743
	-	0.4	0.4	0.2	-	1.05	105.88	2.8162
VIII	0.33	0.33	-	0.33	4.8622	1.02	-	2.8026
	0.2	0.4	-	0.4	4.8622	1.02	-	2.8026
	0.4	0.2	-	0.4	4.8622	1.02	-	2.8026
	0.4	0.4	-	0.2	4.8622	1.02	-	2.8026
IX	0.25	0.25	0.25	0.25	4.9966	1.05	105.88	2.8162
	0.1	0.3	0.3	0.3	4.9966	1.05	105.88	2.8162
	0.3	0.1	0.3	0.3	4.9966	1.05	105.88	2.8162
	0.3	0.3	0.1	0.3	4.9196	1.03	108.92	2.7743
	0.3	0.3	0.3	0.1	4.9966	1.05	105.88	2.8162

for the network planner. For example, if losses are important to the network planner, the coefficient is considered different, although the sum of the coefficients must be equal to 1. Finally, in each of the solved scenarios, a unique answer can be selected from the Pareto set results.

5. CONCLUSIONS

In this paper, the effects of wildfire smoke on the power system were studied. Wildfires are one of the most pervasive events that can affect power system resilience. To reduce this effect, a suitable solution should be considered. so, the effects of wildfires smoke on power system have been investigated based on the wind rose curves on the test power system By solving an example, was shown that many scenarios caused by wind uncertainty can be reduced (for instance three scenarios), and also the optimal placement of distributed generation resources can be very effective in improving the resilience of power systems. It should be noted that a new optimization algorithm has been presented for the first time that is called the handball championship cup algorithm or HCCA algorithm. Based on the proposed method, the optimal location of the distributed generation resources is

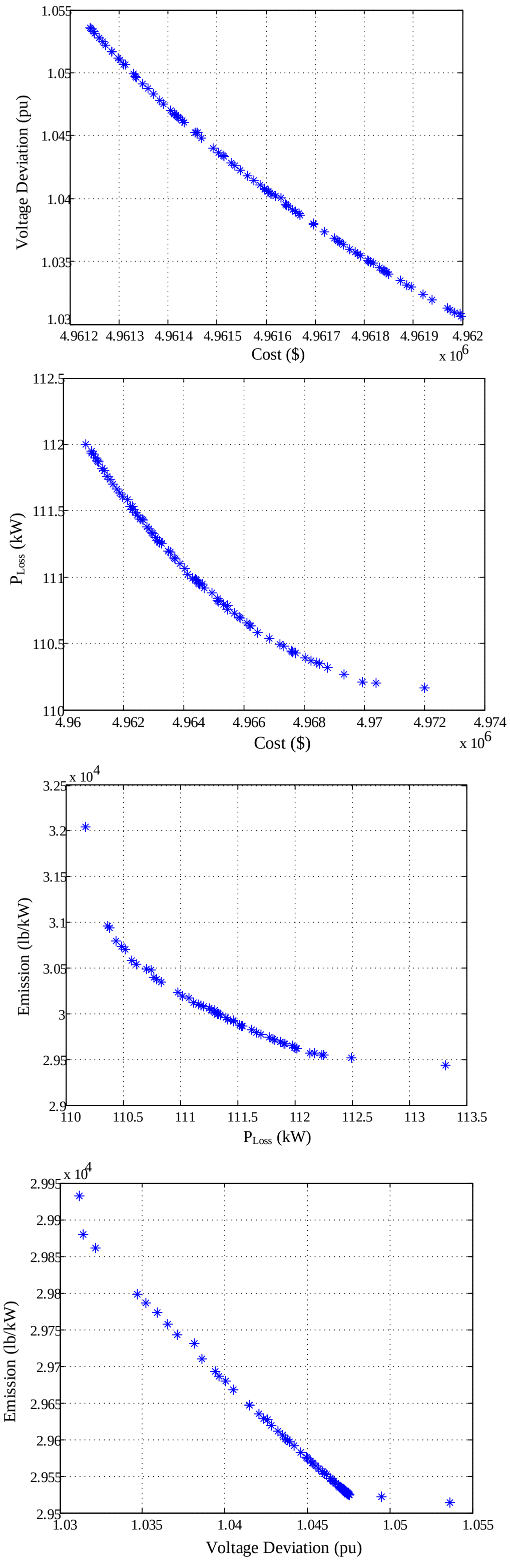

Fig. 10. Pareto front results of objective functions.

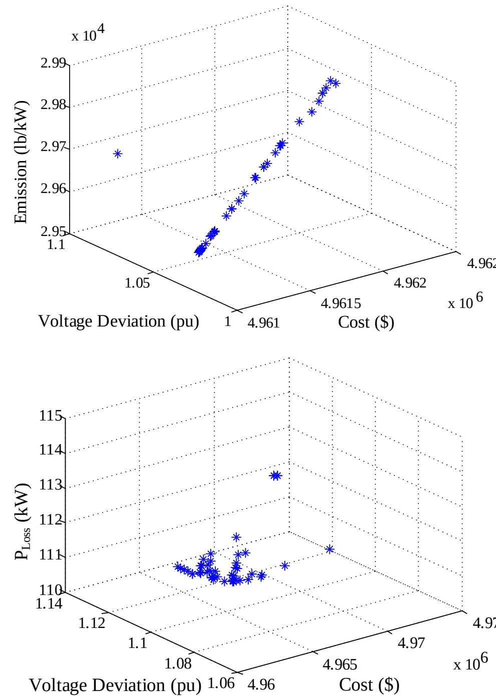

Fig. 11. Three dimension results of objective functions.

Table 7. Objective function values for the third scenario.

Cases	Operational weights W_1	W_2	W_3	W_4	$f_4 * 10^4$ (lb/MW)	f_3 (kW)	f_2 (pu)	$f_1 * 10^6$ ($)
I	-	-	-	-	4.8216	1.15	123.27	3.2303
II	-	-	-	-	5.0108	0.99	120.46	2.6994
III	-	-	-	-	5.0819	1.07	105.38	3.0539
IV	-	-	-	-	5.1469	1.01	112.43	2.6658
V	0.33	0.33	0.33	-	5.0313	1.06	106.38	-
	0.2	4	0.4	-	5.0313	1.06	106.38	-
	0.4	0.2	0.4	-	5.0313	1.06	106.38	-
	0.4	0.4	0.2	-	4.879	1.04	110.09	-
VI	0.33	-	0.33	0.33	4.8419	-	106.17	2.9032
	0.2	-	0.4	0.4	4.8419	-	106.17	2.9032
	0.4	-	0.2	0.4	4.8419	-	106.17	2.9032
	0.4	-	0.4	0.2	4.8419	-	106.17	2.9032
VII	-	0.33	0.33	0.33	-	1.06	106.38	2.8186
	-	0.2	0.4	0.4	-	1.06	106.38	2.8186
	-	0.4	0.2	0.4	-	1.04	110.09	2.7073
	-	0.4	0.4	0.2	-	1.06	106.38	2.8186
VIII	0.33	0.33	-	0.33	4.7439	1.03	-	2.7411
	0.2	0.4	-	0.4	4.7439	1.03	-	2.7411
	0.4	0.2	-	0.4	4.7439	1.03	-	2.7411
	0.4	0.4	-	0.2	4.7439	1.03	-	2.7411
IX	0.25	0.25	0.25	0.25	5.0313	1.06	106.38	2.8186
	0.1	0.3	0.3	0.3	5.0313	1.06	106.38	2.8186
	0.3	0.1	0.3	0.3	5.0313	1.06	106.38	2.8186
	0.3	0.3	0.1	0.3	4.879	1.04	110.09	2.7073
	0.3	0.3	0.3	0.1	5.0313	1.06	106.38	2.8186

easily determined. It is shown that the proposed algorithm has good accuracy, and is suitable for solving the problem of this paper. Also, the results show the power system resilience is increased against the wildfire. Some open issues which are currently the subject of further research include the impact of concurrent smoke and flame and resilience analysis of power system infrastructures against storms by using wind rose curve could be investigated. Also, the insulation failure calculation that is caused by wildfire smoke is one of the issues that should be considered more. Another point is the HCCA algorithm as a new optimization method that could be used in all optimization problems.

REFERENCES

1. H. Farh, A. Al-shaalan, A. Eltamaly, and A. Abdullrahman, " A Novel Crow Search Algorithm Auto-Drive PSO for Optimal Allocation and Sizing of Renewable Distributed Generation," IEEE Access, Vol. 8 , pp. 27807 – 27820, 2020.
2. "Office of President Executive Order, Economic benefits of increasing electric grid resilience to weather outages," U.S. Department of Energy's Office of Electricity Delivery and Energy Reliability, August 2013.
3. R. Campbell, "Weather-related Power Outages and Electric System Resiliency," Congressional Research Service, Library of Congress, pp. 1-8, 2012.
4. Y. Wang, C. Chen, J. Wang, and R. Baldick, "Research on Resilience of Power Systems Under Natural Disasters—A Review," IEEE Transactions on Power Systems, vol. 31, no. 2, pp. 1604-1613, 2016.
5. A. Berkeley, M. Wallace, and C. Coo, "A Framework For Establishing Critical Infrastructure Resilience Goals," Final Report and Recommendations by the Council, National Infrastructure Advisory Council, pp. 18-21, 2010.
6. Z. Bie, Y. Lin, G. Li, and F. Li, "Battling the extreme: a study on the power system resilience,"Proceedings of the IEEE, vol. 105, no. 7, pp. 1253-1264, 2017.
7. M. Panteli, D. Trakas, and P. Mancarella, "Boosting the power grid resilience to extreme weather events using defensive islanding," IEEE Transactions on Smart Grid, vol. 7, no. 6, pp. 2913-2919, 2016.
8. S. Lei, J. Wang, C. Chen, and Y. Hou, "Mobile emergency generator pre-positioning and real-time allocation for resilient response to natural disasters," IEEE Transactions on Smart Grid, vol. 9, no. 3, pp. 2030-2039, 2018.
9. M. Zare, A. Abbaspour, M. Fotuhi-Firuzabad, and M. Moein-Aghtaei, "Increasing the resilience of distribution systems against hurricane by optimal switch placement," in Conference on Electrical Power Distribution Networks Conference (EPDC), 19-20 April 2017, Semnan, Iran, 2017.
10. S. Yao, P. Wang, and T. Zhao, "Transportable energy storage for more resilient distribution systems with multiple microgrids," IEEE Transactions on Smart Grid, vol. 10, no. 3, pp. 3331-3340, 2019.
11. S. Ma; B. Chen; Z. Wang, "Resilience Enhancement Strategy for Distribution Systems under Extreme Weather Events," IEEE Transactions on Smart Grid, vol. 9, no. 2, pp. 1442-1449, 2018.
12. A. Berkeley, M. Wallace, and C. Coo, "A Framework For Establishing Critical Infrastructure Resilience Goals," Final Report and Recommendations by the Council, National Infrastructure Advisory Council, October 2010.
13. D. Cai, X. Li, and Y. Wang, et al., "Impact of natural disasters on the western Hubei power grid and its anti-disaster enhancement measures," The Journal of Engineering, vol. 2019, no. 16, pp. 1976-1980, 2019.
14. M. Mohamed, T. Chen, W. Su and T. Jin, "Proactive Resilience of Power Systems Against Natural Disasters: A Literature Review," IEEE Access, vol. 7, pp. 163778-163795, 2019.
15. P. Karimyan, G.B. Gharehpetian, M. Abedi, and A. Gavili, "Long term scheduling for optimal allocation and sizing of DG unit considering load variations and DG type," International Journal of Electrical Power & Energy Systems, vol. 54, pp. 277-287, 2014.
16. P. Li, D. Huang, J. Ruan, and H. Qin et al., "Influence of Forest Fire Particles on the Breakdown Characteristics of Air Gap," IEEE Transactions on Dielectrics and Electrical Insulation, vol. 23, no. 4, pp. 1974-1983, 2016.
17. K. Charzan, and Z. Wroblebski, "The threat caused by fires under high voltage lines," in 15 st International Conference on Advances in Processing, Testing and Application of Dielectric Materials, Wrocław University of Technology, Wrocław, Poland, Conference 15, no.40, 2014.
18. D. Trakas, and N. Hatziargyriou, "Optimal Distribution Operation For Enhancing Resilience Against Wildfire," IEEE Transactions on Power Systems, vol. 33 , no. 2, pp.1-12, 2018.
19. S. Ma, L. Su, Z. Wang, F. Qiu, and G. Guo, "Resilience enhancement of distribution grids against extreme weather events," IEEE Transactions on Power Systems, vol. 33, no. 5, pp. 4842-4853, 2018.
20. M. Panteli, C. Pickering, and S. Wilkinson, et al., "Power system resilience to extreme weather: fragility modeling, probabilistic impact assessment, and adaptation measures," IEEE Transactions on Power Systems, vol.32, no. 5, pp. 3747–3757, 2017.
21. A. Bagchi, A. Sprintson and C. Singh, "Modeling the impact of fire spread on the electrical distribution network of a virtual city," 41st North American Power Symp, Starkville, MS, USA, pp. 1-6, 2009.
22. M. Choobineh, B. Ansari, and S. Mohagheghi, "Vulnerability assessment of the power grid against progressing wildfires," Fire Safety Journal, vol. 73, pp. 20–28, 2015.
23. S. Mohagheghi, and S. Rebennack, "Optimal resilient power grid operation during the course of a progressing wildfire," International Journal of Electrical Power & Energy Systems, vol. 73, pp. 843-852, 2015.
24. B. Ansari, and S. Mohagheghi, "Optimal energy dispatch of the power distribution network during the course of a progressing wildfire," International Transactions on Electrical Energy Systems, vol. 25, pp. 3422-3438, 2015.
25. M. Salehizadeh, M. Koohbijari, H. Nouri, and A. Taşcıkaraoğlu, et al. "Bi-objective optimization model for optimal placement of thyristor-controlled series compensator devices," Energies, vol. 12, pp. 1-4, 2019.
26. K. Karimizadeh, S. Soleymani, and F. Faghihi, "Optimal placement of DG units for the enhancement of MG networks performance using coalition game theory," IET Generation, Transmission & Distribution , vol. 14 , no. 5, pp. 3-13, 2020.
27. M. Aman, J. Jasmon, H. Mokhlis, and A. Bakar, "Optimal placement and sizing of a DG based on a new power stability index and line losses," International Journal of Electrical Power & Energy Systems, vol. 43, no. 1, pp. 1296-1304, 2012.
28. S. Naik, D. Khatod, and M. Sharma, "Optimal allocation of combined DG and capacitor for real power loss minimization in distribution networks," International Journal of Electrical Power & Energy Systems, vol. 53, pp. 967-970, 2013.
29. A. Abou.El-Ela, S. Allam, and M. Shatla, "Maximal optimal benefits of distributed generation using genetic algorithms," Electric Power System Research, vol. 80, no. 7, pp. 869–877, 2010.
30. M. Moradi, and M. Abedini, "A combination of genetic algorithm and particle swarm optimization for optimal dg location and sizing in distribution systems," International Journal of Electrical Power & Energy Systems, vol. 34, no. 1, pp. 66-72, 2012.
31. C. Tymstra, B. Stocksb, X. Caia, and M. Flannigan, "Wildfire management in Canada: Review, challenges and opportunities," Progress in Disaster Science, vol.5, 2020.
32. Sh. Guan, D.Wong, Y. Gao, T. Zhang, and G. Pouliot, "Impact of wildfire on particulate matter in the southeastern United States in November 2016," Science of The Total Environment, vol. 724, 2020.
33. I. Silvab, M. Vallea, L. Barrosa, and J. Meyer, "A wildfire warning system applied to the state of Acre in the Brazilian Amazon," Applied Soft Computing, vol. 89, 2020.
34. M. Salehizadeh, and S. Soltanian, "Application of fuzzy Q-learning for electricity market modeling by considering renewable power penetration," Renewable and Sustainable Energy Reviews, vol. 56, pp. 1172-1176, 2016.
35. R. Liang, and J. Liao, "A fuzzy-optimization approach for generation scheduling with wind and solar energy systems," IEEE Transactions on Power Systems, vol. 22, no. 4, pp. 1665-1674, 2007.
36. M. Abdi-Siab, and H. Lesani, "Two-stage scenario-based DEP incorpo-

rating PEV using Benders' decomposition," IET Generation, Transmission & distribution, vol. 14, no. 8, pp. 1508-1520, 2020.

37. N. Amjady, J. Aghaei, and H.A. Shayanfar, "Stochastic multiobjective market clearing of joint energy and reserves auctions ensuring power system security," IEEE Transactions on Power Systems, vol. 24, no. 4, pp. 1841-1850, 2009.
38. F. Castellani, A. Garinei, L. Terzi, D. Astolfi, and M. Gaudiosi, "Improving wind farm operation practice through numerical modelling and supervisory control and data acquisition data analysis," IET Renewable Power Generation, vol. 8 , no. 4 , pp.367-373, 2014.
39. N. Duan, W. Xu, T. Yuan, and S. Wang, et al., " Modelling of Hysteresis Phenomenon Based on the Elemental Operator and Wind-Rose Method," in 21st International Conference on Electrical Machines and Systems (ICEMS), 7-10 Oct. 2018, Jeju, South Korea, 2018.
40. S. Chavan, V. Saahil, A. Singh, and H. Himanshu, et al., "Application of wind rose for wind turbine installation," International Conference on Circuit ,Power and Computing Technologies (ICCPCT), 19 October 2017, Kollam, India, 2017.
41. A. Leporea, B. Palumbo, and A. Pievatolo, "A Bayesian approach for site-specific wind rose prediction," Renewable Energy, vol. 150, pp. 691-702, 2020.
42. N. Arreyndip, and E. Joseph, "Small 500 kW onshore wind farm project in Kribi, Cameroon: Sizing and checkers layout optimization model," Energy Reports, vol. 4, pp. 528-535, 2018.
43. "Local weather information of high quality worldwide for any point on land or sea in the world ", Available: www.meteoblue.com [Accessed: Nov. 23, 2020].
44. N. Javidtash, M. Jabbari, T. Niknam, and M. Nafar, "A novel mixture of non-dominated sorting genetic algorithm and fuzzy method to multi-objective placement of distributed generations in Microgrids," Journal of Intelligent and Fuzzy Systems, vol. 33, no.4, pp. 2577-2584, 2017.
45. "International Handball Federation," Available: www.ihf.info [Accessed: Nov. 23, 2020].
46. E. Almabsout, R. El-Sehiemy, O. Nuri, and O. Bayat, "A Hybrid Local Search-Genetic Algorithm for Simultaneous Placement of DG Units and Shunt Capacitors in Radial Distribution Systems," IEEE Access, vol. 8, pp. 54465 - 54481, 2020.
47. H. Doagoo-Mojarrad, G.B. Gharepetian, H. Rastegar, J. Olamaei, "Optimal placement and sizing of DG (distributed generation) units in distribution networks by novel hybrid evolutionary algorithm," Energy, vol. 54, pp. 129-138, 2013.
48. T. Niknam, I. Taheri, J. Aghaei, S. Tabatabaei, M. Nayeripour, "A modified honey bee mating optimization algorithm for multiobjective placement of renewable energy resources," Applied Energy, vol. 88, no.12, PP. 4818-4821, 2011.
49. C.A.S. Coello, G.T. Pulidio, and M.S. Salazar, "Handling Multiple Objectives With Particle Swarm Optimization," IEEE Transactions on Evolutionary Computation, vol. 8, no. 3, pp. 256-268, 2004.

6. APPENDIX

To show the performance of the HCCA algorithm, four benchmark functions that are presented in the MOPSO algorithm paper by Coello are presented as follows [49]:

The first test function is:

$$F1 = -x^2 + y \tag{36}$$

$$F2 = \frac{1}{2}x + y + 1 \tag{37}$$

$$0 \geq \frac{1}{6}x + y - \frac{13}{2} \& \; 0 \geq \frac{1}{2}x + y - \frac{15}{2} \tag{38}$$

$$0 \geq 5x + y - 30 \; \& \; 0 \leq x, y \leq 7 \tag{39}$$

The second test function is:

$$F1 = \sum_{i=1}^{n-1} \left(-10 \exp\left(-0.2\sqrt{x_i^2 + x_{i+1}^2} \right) \right) \tag{40}$$

$$F2 = \sum_{i=1}^{n} \left(|x_i|^{0.8} + 5\sin(x_i)^3 \right) \tag{41}$$

$$-5 \leq x_1, \; x_2, x_3 \leq +5 \tag{42}$$

The third test function is:

$$Minimize[f_1(x_1, x_2)] = x_1 \tag{43}$$

$$Minimize[f_2(x_1, x_2) = g(x_1, x_2) . h(x_1, x_2)] \tag{44}$$

$$h(x_1, x_2) = \begin{cases} 1 - \sqrt{\frac{f_1(x_1,x_2)}{g(x_1,x_2)}} \; if \; f_1(x_1, x_2) \leq g(x_1, x_2) \\ 0, \qquad otherwise \end{cases} \tag{45}$$

$$g(x_1, x_2) = 11 + x_2^2 - 10\,(\cos 2\pi x_2) \tag{46}$$

$$0 \leq x_1 \leq 1\& \; -30 \leq x_2 \leq 30 \tag{47}$$

The fourth test function is:

$$Minimize[f_1(x_1, x_2) = x_1] \tag{48}$$

$$Minimize[f_2(x_1, x_2) = \frac{g(x_2)}{x_1}] \tag{49}$$

$$g(x_2) = 2.0 - exp\left\{-\left(\frac{x_2-0.2}{0.004}\right)^2\right\} -0.8\,exp\left\{-\left(\frac{x_2-0.6}{0.4}\right)^2\right\} \tag{50}$$

$$0.1 \leq x_1, \; x_2 \leq 1 \tag{51}$$

The comparison between HCCA and MOPSO algorithms for the first and the second test functions are shown in Figs. 12 and 13 and also numerical results of the comparison between HCCA, MOPSO, and NSGA-II algorithms for the third and fourth test functions are presented in Tables 8-11.

Table 8. Results of the generational distance for the third test function.

GD	HCCA	MOPSO	NSGA-II
Mean	0.0001097	0.000118	0.023046
Std Dev	$2.372 * 10^{-5}$	$2.55 * 10^{-5}$	0.045429

Table 9. Computational time (in second) for the third test function.

Time	HCCA	MOPSO	NSGA-II
Mean	0.104545	0.0721	0.69355
Std Dev	0.011368	0.00784	0.020028

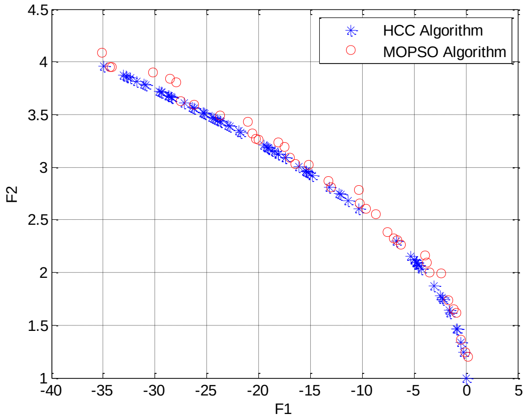

Fig. 12. Comparison between HCCA and MOPSO algorithms for the first test function.

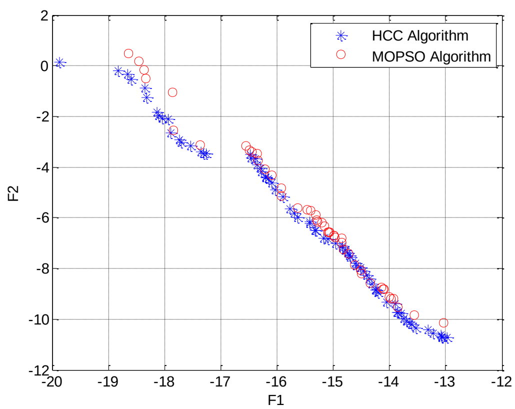

Fig. 13. Comparison between HCCA and MOPSO algorithms for the second test function.

Table 10. Results of the generational distance for the fourth test function.

GD	HCCA	MOPSO	NSGA-II
Mean	0.0301116	0.03273	0.044236
Std Dev	0.0557704	0.06062	0.07368

Table 11. Computational time (in second) for the third test function.

Time	HCCA	MOPSO	NSGA-II
Mean	0.401288	0.27675	1.578
Std Dev	0.079566	0.054873	0.073463